Turkish J. Eng. Env. Sci.
33 (2009) , 193 – 205.

doi:10.3906/muh-0905-21

Double diffusive mixed convection flow over a moving vertical plate in the presence of internal heat generation and a chemical reaction

P. M. PATIL[1], S. ROY[2], A. J. CHAMKHA[3]
[1]*Department of Mathematics, J S S's Banashankari Arts, Commerce and S. K. Gubbi Science College, Vidyagiri, Dharwad – 580 004, INDIA*
e-mail: dr_pmpatil@yahoo.co.in
[2]*Department of Mathematics, I.I.T. Madras, Chennai, 600 036, INDIA*
e-mail: sjroy@iitm.ac.in
[3]*Manufacturing Engineering Department, The Public Authority for Applied Education and Training, Shuweikh 70654, KUWAIT*
e-mail: achamkha@yahoo.com

Received 20.05.2009

Abstract

This paper investigates the steady, laminar mixed convection flow over a continuously moving semi-infinite vertical plate due to the combined effects of thermal and mass diffusion in the presence of internal heat generation or absorption and an nth order homogeneous chemical reaction between the fluid and the diffusing species. The nonlinear partial differential equations governing the flow, thermal, and concentration fields are obtained in non-similar form by introducing suitable transformations. The final non-similar set of coupled nonlinear partial differential equations is solved using an implicit finite difference scheme in combination with quasilinearization. A parametric study is performed to illustrate the influence of various parameters on the velocity, temperature, and concentration profiles in the present investigation. Further, the numerical results are presented for the skin friction coefficient, Nusselt number, and Sherwood number.

Introduction

Double diffusive convection phenomena involve buoyancy driven flows induced by a combination of temperature and concentration gradients. Double diffusion occurs in a wide range of scientific and technological fields such as oceanography, geology, biology, astrophysics, and chemical processes. Extensive reviews have been reported on the subject by Ostrach (1980) and Viskanta et al. (1985). The behavior of steady boundary layer flow over a moving flat surface with constant velocity was first presented by Sakiadis (1961), who analyzed it theoretically by both analytical and approximate methods. Remarkable differences were found between this behavior and the behavior of the boundary layer in a moving fluid over a steady flat surface, considered by Blasius (1908). Boundary layer flow behavior on a moving surface is an important type of flow occurring in many engineering and technological processes. The examples of practical applications of continuous surfaces are cooling of an infinite metallic plate in a cooling bath, aerodynamic extrusion of plastic sheets, the boundary layer along a liquid film in condensation processes and a polymer sheet or filament extruded continuously from a dye, or a

long thread travelling between a feed roll and a wind-up roll. A combined analytical and experimental study of the flow and temperature fields in the boundary layer over a continuous moving surface has been carried out by Tsou et al. (1967). In their study, the authors showed that an analytically describable boundary layer on the continuous moving surface is a physically realizable flow.

Following Blasius and Sakiadis, Abdelhafez (1985) studied the boundary layer flow on a moving flat surface to a parallel free stream, and the case when the surface and the free stream move in the same direction with constant velocity was considered. He presented that the studies by Blasius and Sakiadis are 2 special cases of his work. Chappidi and Gunnerson (1989) considered a similar problem, and presented an analytical solution. Afzal et al. (1993) formulated a single set of boundary conditions, employing a composite reference velocity$U = U_W + U_\infty$, where U_W is wall velocity and $U_\infty$is the free stream velocity, instead of considering U_W and U_∞separately as it was considered by Abdelhafez (1985), and Chappidi and Gunnerson (1989).

Furthermore, Afzal et al. (1993) analyzed the case when the wall and the free stream move in opposite directions, and showed that dual solutions exist. Lin and Haung (1994) analyzed a horizontal isothermal plate moving in parallel or reversibly to a free stream where similarity and non-similarity equations are used to obtain the flow and thermal fields. The detailed analyses of the problem of laminar fluid flow that results from the combined motions of a bounding surface and free stream in the same direction have been discussed by Abraham and Sparrow (2005) and Sparrow and Abraham (2005) using the relative velocity model, which uses the magnitude of the relative velocity in conjunction with the drag formula for the case in which only one of the participating media is in motion. Recently, Cortell (2007) extended the work of Afzal et al. (1993), by taking into account the effect of viscous dissipation in the energy equation. The effects of transpiration on the flow and heat transfer over a moving permeable surface in a parallel stream were analyzed by Ishak et al. (2009). Ishak et al. (2007) examined the boundary layer flow over a continuously moving thin needle in a parallel stream. The development of the boundary layer on a fixed or moving surface parallel to a uniform free stream in presence of surface heat flux has been investigated by Ishak et al. (2009).

The main objective of the present analysis was to investigate the effect of heat and mass transfer in a mixed convection flow over a moving vertical surface parallel to a free stream in presence of heat generation or absorption and an nth order homogeneous chemical reaction between the fluid and the diffusing species. The coupled non-linear partial differential equations governing the flow have been solved numerically using an implicit finite difference method in combination with quasilinearization (Inouye, 1974; Roy and Saikrishnan, 2003).

Mathematical Formulation

Consider a steady incompressible viscous heat generating or absorbing mixed convection boundary layer flow along a semi-infinite vertical plate moving with velocity U_W in the x- direction. The x-axis is taken along the plate in the vertically upward direction and the y-axis is taken normal to it. Figure 1 shows the coordinate system and physical model for the flow configuration. The free stream velocity U_∞ and plate velocity $U_W$are constants in the same direction. The surface is maintained with prescribed wall temperature T_w different from the porous medium temperature T_∞sufficiently away from the surface. A heat source is placed within the flow to allow possible heat generation or absorption effects. The concentration of diffusing species is assumed to be very small in comparison with other chemical species far from the surfaceC_∞, and is infinitely small. Hence the Soret and Dufour effects are neglected. The buoyancy force arises due to the temperature difference in

the fluid. The nth order homogeneous chemical reactions are taking place in the flow. All thermophysical properties of the fluid in the flow model are assumed constant except for the density variations causing a body force in the momentum equation. The Boussinesq approximation is invoked for the fluid properties to relate density changes, and to couple in this way the temperature field to the flow field (Schlichting, 2000). Under these assumptions, the equations of conservation of mass, momentum, energy, and concentration governing the mixed convection boundary layer flow over a moving vertical plate are given by:

$$\frac{\partial u}{\partial x} + \frac{\partial v}{\partial y} = 0, \tag{1}$$

$$u\frac{\partial u}{\partial x} + v\frac{\partial u}{\partial y} = \nu\frac{\partial^2 u}{\partial y^2} \pm g\beta_T\,(T - T_\infty) \pm g\beta_C\,(C - C_\infty), \tag{2}$$

$$u\frac{\partial T}{\partial x} + v\frac{\partial T}{\partial y} = \alpha\frac{\partial^2 T}{\partial y^2} \pm \frac{Q_0}{\rho C_p}\,(T - T_\infty), \tag{3}$$

$$u\frac{\partial C}{\partial x} + v\frac{\partial C}{\partial y} = D\frac{\partial^2 C}{\partial y^2} - k_1\,(C - C_\infty)^n, \tag{4}$$

where all the parameters are defined in the nomenclature. It should be mentioned here that for homogeneous-type chemical reactions a single term in Eq. (4) is obtained. However, if the chemical reaction is heterogeneous, the change will be in the boundary conditions.

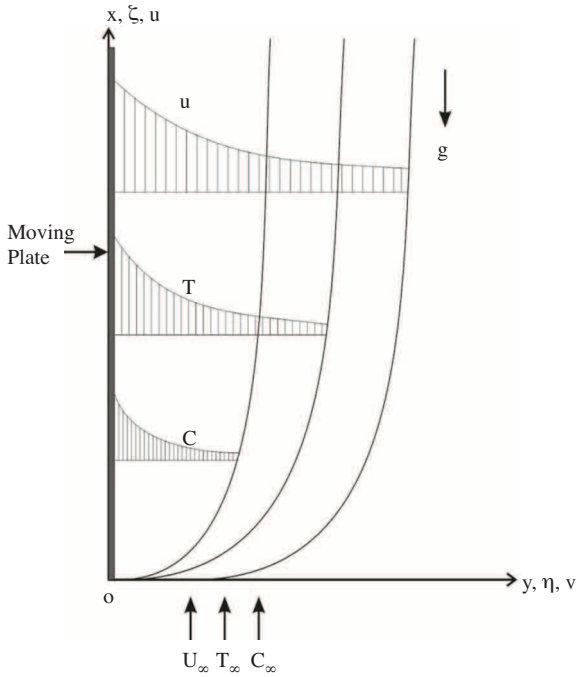

Figure 1. Physical model and coordinate system.

The physical boundary conditions are given by:

$$y = 0: \quad u = U_W, \quad v = 0, \quad T = T_W, \quad C = C_W,$$

$$y \to \infty : \quad u \to U_\infty, \qquad T = T_\infty, \quad C = C_\infty. \tag{5}$$

Applying the following transformations:

$$\xi = \frac{x}{L}; \quad \eta = \left(\frac{U}{\nu x}\right)^{\frac{1}{2}} y; \quad \psi(x,y) = (\nu U x)^{\frac{1}{2}} f(\xi,\eta); \quad u = \frac{\partial \psi}{\partial y}; \quad v = -\frac{\partial \psi}{\partial x};$$

$$u = U f_\eta, \quad U = U_\infty + U_w; \quad v = -\frac{(\nu x U)^{\frac{1}{2}}}{2x}\{f(\xi,\eta) + \xi f_\xi - \eta f_\eta\}; \quad T - T_\infty = (T_W - T_\infty)\,\Theta(\xi,\eta);$$

$$(C - C_\infty) = (C_W - C_\infty)\,\Phi(\xi,\eta); \quad Gr = \frac{g\beta_T (T_W - T_\infty) L^3}{\nu^2}; Gr^* = \frac{g\beta_C (C_W - C_\infty) L^3}{\nu^2}; \quad \lambda = \frac{Gr}{Re_L^2};$$

$$\lambda_1 = \frac{Gr^*}{Re_L^2}; \quad Re_L = \frac{UL}{\nu}; \quad N = \frac{\lambda_1}{\lambda}; \quad \Pr = \frac{\nu}{\alpha}; \quad Q = \frac{Q_0 L}{\rho C_p U}; \quad Sc = \frac{\nu}{D}; \quad \Delta = \frac{k_1 (C_W - C_\infty)^{n-1} L}{U}; \tag{6}$$

to Eqs. (1)-(4), we find that Eq. (1) is satisfied identically, and Eqs. (2)-(4) reduce to

$$F_{\eta\eta} + \frac{f}{2} F_\eta \pm \lambda\xi(\Theta + N\Phi) = \xi(F F_\xi - f_\xi F_\eta), \tag{7}$$

$$\Theta_{\eta\eta} + \frac{\Pr f}{2}\Theta_\eta \pm \Pr Q\xi\Theta = \Pr\xi(F\Theta_\xi - f_\xi\Theta_\eta) \tag{8}$$

$$\Phi_{\eta\eta} + \frac{Scf}{2}\Phi_\eta - Sc\Delta\xi\Phi^n = Sc\xi(F\Phi_\xi - f_\xi\Phi_\eta), \tag{9}$$

where $f = \int_0^\eta F d\eta + f_w; f_w = 0$ (F here is the derivative of f. That is F = f'). It should be noted that f_w is taken to be zero since the plate is impermeable. That is, there is no suction or injection.

The above set of transformations changes the non-linear coupled partial differential equations (1)-(3) into dimensionless form as Eqs. (7)-(9). However, these transformations do not reduce the number of independent variables and such cases are known as non-similar transformations (Schlichting, 2000). In Eq. (7), λ that represents the buoyancy force effect on the flow field has $\pm$ signs; the plus sign indicates the buoyancy-upward (or buoyancy assisted) flow, while the negative sign stands for buoyancy-downward (or buoyancy opposed) flow. When $T_w > T_\infty$ and $T_w < T_\infty$, opposite signs are produced because the buoyancy force is assisting the flow and in the other case it opposes the flow.

The non-dimensional boundary conditions become:

$$F = 1 - \varepsilon, \quad \Theta = 1, \quad \Phi = 1, \text{ at } \eta = 0,$$
$$F \to \varepsilon, \quad \Theta \to 0, \quad \Phi \to 0, \text{ as } \eta \to \infty \tag{10}$$

where $\varepsilon = \frac{U_\infty}{U_\infty + U_w}$corresponds to the ratio of free stream velocity to the composite reference velocity. The momentum Eq. (7) is coupled with all the other equations of the system. The ratio of buoyancy forces N appearing in Eq. (7) is the non-dimensional parameter representing the ratio between the buoyancy force due to concentration difference and the buoyancy force due to temperature difference. N is zero for no buoyancy effect due to mass diffusion, is infinite for no buoyancy effect due to thermal diffusion, is unity for thermal

and mass buoyancy forces of the same strength, is positive (>0) for the combined buoyancy forces driving the flow, and is negative (<0) for the buoyancy forces opposing each other. The heat generation or absorption parameter Q appearing in Eq. (8) is the non-dimensional parameter based on the amount of heat generated or absorbed per unit volume given by $Q_0\,(T - T_\infty)$, with Q_0 being a constant coefficient that may take either positive or negative values. The source term represents the heat generation that is distributed everywhere when $Q$is positive (>0) and the heat absorption when Q is negative (<0). Q is zero in the case of no heat source. The chemical reaction parameter Δ appearing in Eq. (9) is the non-dimensional parameter representing the generation or consumption of the diffusing species. The chemical reaction parameter Δ is positive (>0) for species generation, is negative (<0) for species consumption, and is zero for no chemical reaction.

The local skin friction coefficient C_{fx} is defined as:

$$C_{fx} = \mu \frac{\partial u/\partial y}{\frac{1}{2}\rho U^2} = 2Re_L^{-\frac{1}{2}} \xi^{-\frac{1}{2}} F_\eta\,(\xi, 0)\,, \text{ i.e. } C_{fx} Re_L^{\frac{1}{2}} = 2F_\eta \xi^{-\frac{1}{2}}\,(\xi, 0)\,. \tag{11}$$

The local heat transfer rate in terms of the Nusselt number can be expressed as:

$$Nu_x = -x \frac{\partial T/\partial y}{(T_w\,(x) - T_\infty)} = -Re_L^{\frac{1}{2}} \xi^{\frac{1}{2}} \Theta_\eta\,(\xi, 0)\,, \text{ i.e. } Nu_x Re_L^{-\frac{1}{2}} = -\Theta_\eta \xi^{\frac{1}{2}}\,(\xi, 0)\,. \tag{12}$$

The local mass transfer rate in terms of the Sherwood number can be expressed as:

$$Sh_x = -x \frac{\partial C/\partial y}{(C_w\,(x) - C_\infty)} = -Re_L^{\frac{1}{2}} \xi^{\frac{1}{2}} \Phi_\eta\,(\xi, 0)\,, \text{ i.e. } Sh_x Re_L^{-\frac{1}{2}} = -\Phi_\eta \xi^{\frac{1}{2}}\,(\xi, 0)\,. \tag{13}$$

Method of solution

Non-linear coupled partial differential equations (7)-(9) under the boundary conditions (10) have been solved numerically using an implicit finite difference scheme in combination with the quasilinearization technique (Inouye, 1974; Roy and Saikrishnan, 2003). An iterative sequence of linear equations was carefully constructed to approximate the non-linear equations (7)-(9) for achieving quadratic convergence and monotonicity. Using the quasilinearization technique, the non-linear partial differential equations are replaced by a sequence of linear partial differential equations at each iteration step. Solutions of this sequence of partial differential equations form a monotone sequence at each nodal point. The errors in the solutions at any 2 successive iterations reduce quadratically. Thus, the sequence converges quadratically to the exact solutions. Upon using the quasilinearization technique, the nonlinear coupled partial differential equations (7)-(9) with boundary conditions (10) are replaced by the following sequence of linear partial differential equations:

$$F_{\eta\eta}^{i+1} + A_1^i F_\eta^{i+1} + A_2^i F^{i+1} + A_3^i F_\xi^{i+1} + A_4^i \Theta^{i+1} + A_5^i \Phi^{i+1} = A_6^i \tag{14}$$

$$\Theta_{\eta\eta}^{i+1} + B_1^i \Theta_\eta^{i+1} + B_2^i \Theta^{i+1} + B_3^i \Theta_\xi^{i+1} + B_4^i F^{i+1} = B_5^i, \tag{15}$$

$$\Phi_{\eta\eta}^{i+1} + C_1^i \Phi_\eta^{i+1} + C_2^i \Phi^{i+1} + C_3^i \Phi_\xi^{i+1} + C_4^i F^{i+1} = C_5^i. \tag{16}$$

The coefficient function with iterative index $i$is known and the function with iterative index $(i+1)$ is to be determined. The corresponding boundary conditions are given by

$$\begin{array}{llll} F^{i+1} = 1 - \varepsilon, & \Theta^{i+1} = 1, & \Phi^{i+1} = 1, & \text{at } \eta = 0 \\ F^{i+1} \to \varepsilon, & \Theta^{i+1} \to 0, & \Phi^{i+1} \to 0, & \text{as } \eta \to \eta_\infty. \end{array} \tag{17}$$

The coefficients in Eqs. (10)-(16) are given by

$$A_1^i = \frac{f}{2} + \xi f_\xi; A_2^i = -\xi F_\xi; \quad A_3^i = -\xi F; A_4^i = \lambda\xi; \quad A_5^i = \lambda\xi N; \quad A_6^i = -\xi F F_\xi;$$

$$B_1^i = \Pr\left(\frac{f}{2} + \xi f_\xi\right); B_2^i = \Pr Q\xi; B_3^i = -\Pr \xi F; B_4^i = -\Pr \xi\Theta_\xi; B_5^i = -\Pr \xi F\Theta_\xi;$$

$$C_1^i = Sc\left(\frac{f}{2} + \xi f_\xi\right); C_2^i = -nSc\xi\Delta\Phi^{n-1}; C_3^i = -Sc\xi F; C_4^i = -Sc\xi\Phi_\xi; \quad C_5^i = -Sc\xi\,(n-1)\,\Delta\Phi^n - Sc\xi\Phi_\xi F.$$

Since the method is presented for ordinary differential equations by Inouye and Tate (1974) and also presented for partial differential equations by Roy and Saikrishnan (2003), its detailed description is not provided here. The non-similar equations (7)-(9) are linearized and then descritized using 3-point central-difference quotients and using 2-point backward difference formulae in the ξ direction. The resulting equations form a tri-diagonal system of algebraic equations that can be solved by Varga's algorithm (2000). The solution process starts at $\xi = 0$ for which Eqs. (7)-(9) become ordinary self-similar equations that can be readily solved. Having the solution at $\xi = 0$ allows the solution of the non-similar equations to march forward in the ξ direction. This is why the 2-point backward difference is used for the ξ-derivative terms regardless of assisting or opposing flow conditions. Therefore, the solutions starts at $\xi = 0$ and then marches forward using the solution at the previous line of constant ξ until it reaches the desired value of ξ. To ensure the convergence of the numerical solution to the exact solution, constant step sizes $\Delta\eta$ and $\Delta\xi$ are optimized and taken as 0.01 and 0.001, respectively. The results presented here are independent of the step sizes at least up to the fourth decimal place. A convergence criterion based on the relative difference between the current and previous iteration values is employed. When the difference reaches 0.00001, the solution is assumed to have converged and the iteration process is terminated.

Results and Discussion

Computations have been carried out for various values of $\Pr\,(0.7 \le \Pr \le 7.0)$, $\lambda\,(-1.0 \le \lambda \le 5.0)$, $N\,(-1.0 \le N \le 1.0)$, $n\,(1.0 \le n \le 3.0)$, $Sc\,(0.22 \le Sc \le 2.57)$, $\varepsilon\,(0.1 \le \varepsilon \le 0.9)$, $Q\,(-2.0 \le Q \le 2.0)$, and $\Delta\,(-1.0 \le \Delta \le 1.0)$. The edge of the boundary layer(η_∞) has been taken between 4.0 and 9.0 depending on the values of the parameters.

The effects of the buoyancy parameterλ and the parameter ε (the ratio of free stream velocity to the composite reference velocity) on the velocity profile $F(\xi, \eta)$ are displayed in Figure 2. It is observed that, for buoyancy aiding flow ($\lambda > 0$), the buoyancy force shows significant overshoot in the velocity profiles near the wall for the parameter ε. The physical reason is the combined effects of assisting buoyancy force due to thermal and concentration gradients and heat generation acts like a favorable pressure gradient that enhances the fluid acceleration. The magnitude of the overshoot decreases in buoyancy opposing flow ($\lambda < 0$). The velocity is strongly depending on ε because it occurs in the boundary condition for $F(\xi, \eta)$.

The effects of the ratio of buoyancy forces (N) and the Prandtl number (Pr) on the velocity profile $F\,(\xi, \eta)$ are presented in Figure 3. In the ratio of buoyancy forces aiding flow($N > 0$), the buoyancy forces show significant overshoot in the velocity profiles near the wall for a lower Prandtl number (Pr) fluid, whereas the velocity overshoot is not present for a higher Prandtl number fluid. Although the magnitude of the overshoot increases with the ratio of buoyancy forces parameter $N\,(N > 0)$, it decreases as the Prandtl number (Pr)

increases. The physical reason is that the ratio of buoyancy forces parameter N affects more in the smaller Prandtl number fluid (Air, $Pr = 0.7$) due to the lower viscosity of the fluid. Hence, the velocity increases within the moving boundary layer as the assisting buoyancy force acts like a favorable pressure gradient and velocity overshoot occurs. For higher Prandtl number fluids the overshoot is not present because of the higher Prandtl number (Pr) (water, $Pr = 7.0$) with more viscous fluid, which makes it less sensitive to the buoyancy force. It is interesting to note from Figure 3 that for the ratio of buoyancy opposing flow, i.e. ($N < 0$), the buoyancy opposing force reduces the magnitude of the velocity significantly within the boundary layer for low Prandtl number fluid ($Pr = 0.7$, air) as well as for high Prandtl number fluid ($Pr = 7.0$, water).

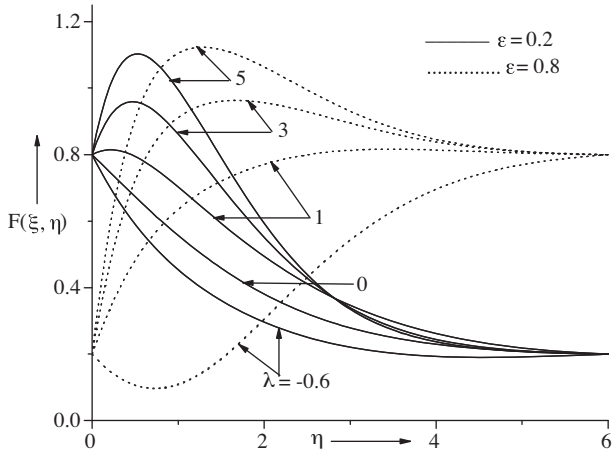

Figure 2. Effects of λ and ε on velocity profile for $\xi = 0.5$, $Pr = 7.0$, $N = 0.5$, $n = 1.0$, $Q = 0.5$, $Sc = 022$ and $\Delta = 0.5$.

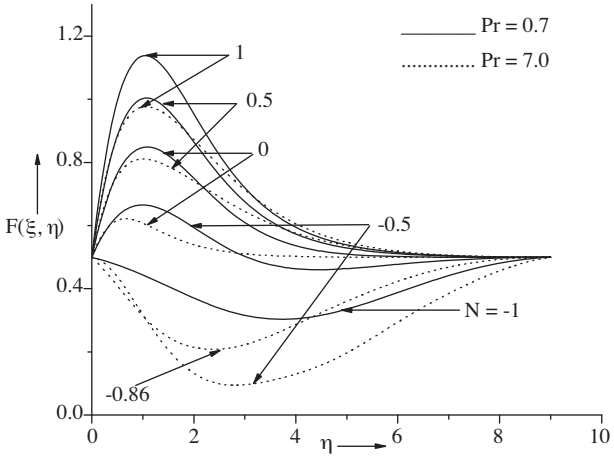

Figure 3. Effects of N and Pr on temperature profile for $\lambda = 2$, $\Delta = 0.5$, $n = 1$, $Q = 0.5$, $\varepsilon = 0.5$, $\xi = 0.5$, and $Sc = 0.22$.

The effects of the ratio of buoyancy forces parameter (N) and Prandtl number Pr on temperature profile $\Theta(\xi, \eta)$ are shown in Figure 4. The results indicate that an increase in the (higher) Prandtl number (Pr) (water, $Pr = 7.0$) clearly induces a strong reduction in the temperature of the fluid and thus results in a thinner thermal boundary layer. Prandtl number Pr is inversely proportional to thermal conductivity and as such lower Pr fluids will possess higher thermal conductivities and therefore diffuse heat energy more than momentum.

Figure 5 illustrates the influence of the heat generation or absorption parameter Q on the temperature profile for $\lambda = 1.0$, $Sc = 0.22$, $N = 1.0$, $n = 1.0$, $\Delta = 0.5$, $\xi = 1.0$, and $\varepsilon = 0.5$. It is noted that, owing to the presence of a heat generation or a heat source effect ($Q > 0$), the thermal state of the fluid increases. Hence, the temperature of the fluid increases within the boundary layers. In the event that the strength of the heat source is relatively large, the overshoot is observed in the temperature profiles within the thermal boundary layer as can be seen in Figure 5. Further, the effect of heat generation is more pronounced on temperature profiles for high Prandtl number fluids ($Pr = 7.0$, water). Figure 5 displays that for $Pr = 7.0$ the temperature profile has approximately 20% overshoot with a thin thermal boundary layer due to higher thermal conductivity. Conversely, the presence of heat absorption or a heat sink effect ($Q < 0$) has the tendency to reduce the fluid temperature. This causes the thermal buoyancy effects to decrease, resulting in a net reduction in the fluid velocity. These behaviors are clearly observed in Figure 5 in which the magnitude of temperature field decreases for $Q < 0$. Moreover, it is also observed that the thickness of the thermal (temperature) boundary layer decreases as the heat absorption

or heat sink effect increases.

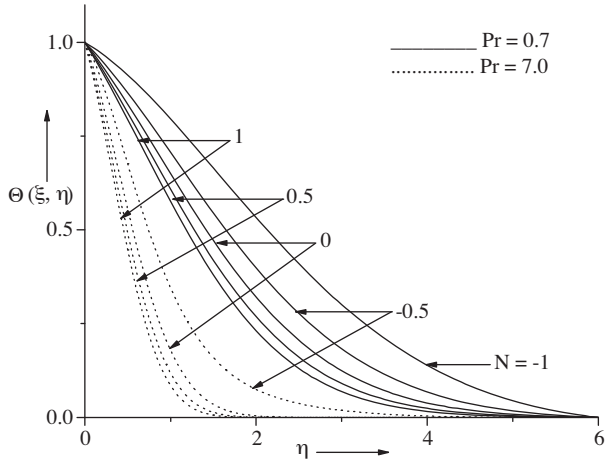

Figure 4. Effects of N and Pr on temperature profile for $\lambda = 2$, $\Delta = 0.5$, $n = 1$, $Q = 0.5$, $\varepsilon = 0.5$, $\xi = 0.5$, and $Sc = 0.22$.

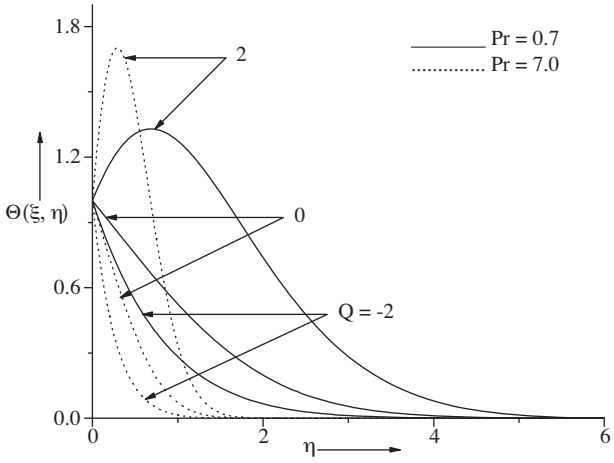

Figure 5. Effects of Q and Pr on temperature profile for $\lambda = 1$, $N = 1$, $n = 1$, $\Delta = 0.5$,, $\varepsilon = 0.5$, and $Sc = 0.22$.

Figure 6 depicts the influence of the chemical reaction parameter Δ on the dimensionless concentration $\Phi(\eta)$ profile. The values of the Schmidt number (Sc) are chosen to be more realistic, 0.22, 0.94, 2.57, representing diffusing chemical species of most common interest like water, propyl benzene hydrogen, water vapor, and propyl benzene, at 25 °C at 1 atmospheric pressure. It shows that the magnitude of the concentration distributions decrease when the chemical reaction parameter $|\Delta|$ (species consumption or destructive chemical reaction) is increased. An increase in the concentration of the diffusing species increases the mass diffusion and thus, in turn, the fluid velocity and temperature increase. In contrast, for $\Delta > 0$ (species generation or constructive chemical reaction), as Δ increases the velocity distribution decreases, so that the concentration falls.

Figure 7 illustrates the influence of the Schmidt number Sc and order of chemical reaction parameter n on dimensionless concentration $\Phi(\eta)$ profiles. It is observed that the concentration and velocity boundary layers decrease as the Schmidt number Sc is increased. Further, it is observed that the thickness of the boundary layer increases as the order of chemical reaction parameter n increases. The physical reason is that the Schmidt number Sc leads to a thinning of the concentration boundary layer while the order of chemical reaction parameter n leads to thickening of the concentration boundary layer. As a result, the concentration of the fluid decreases and this leads to a decrease in the fluid velocity. This is similar to the effect of increasing Prandtl number Pr on the thickness of a thermal boundary layer.

The effects of N (the ratio of buoyancy forces) and Prandtl number Pr on the skin friction coefficient $\left(C_{fx}Re_L^{1/2}\right)$ when $\lambda = 2.0$, $n = 1.0$, $\varepsilon = 0.5$, $Sc = 0.22$, $\Delta = 0.5$, and $Q = 0.5$ are shown in Figure 8. The results indicate that the skin friction coefficient $\left(C_{fx}Re_L^{1/2}\right)$ increases with Prandtl number (Pr) for both lower and higher Prandtl number (Pr) fluid monotonously. This is due to the fact that the increase in N enhances the fluid acceleration and hence the skin friction coefficient increases. In particular for $Pr = 0.7$ at $\xi = 1.0$, the skin friction coefficient $\left(C_{fx}Re_L^{1/2}\right)$ increases approximately 76% as N increases from 0.0 to 1.0, while for Pr

= 7.0 the skin friction coefficient $\left(C_{fx}Re_L^{1/2}\right)$ decreases approximately 55% when N decreases from $N = 1.0$ to 0.0.

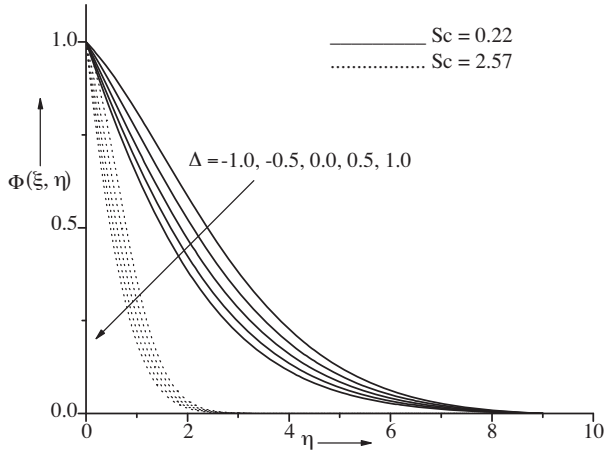

Figure 6. Effects of Δ and Sc on concentration profile for $\lambda = 2$, $N = 1$, $n = 1$, $\Delta = 0.5$, $\varepsilon = 0.5$, and $Pr = 0.7$.

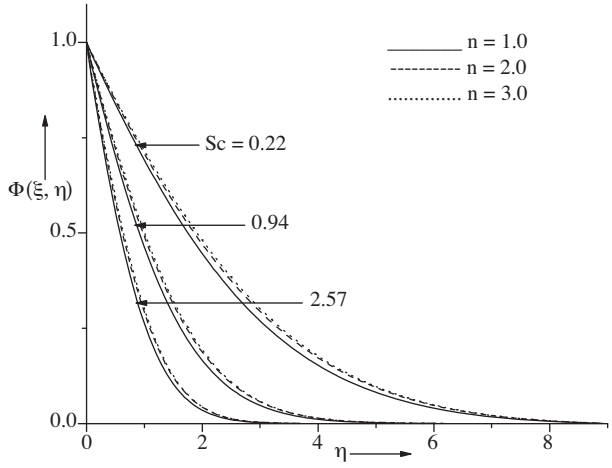

Figure 7. Effects of n and Sc on concentration profile for $\lambda = 2$, $N = 1$, $\Delta = 0.5$, $Q = 0.5$, $\varepsilon = 0.5$, $\xi = 0.5$, and $Pr = 0.7$.

Figure 9 displays the effect of skin friction coefficient $\left(C_{fx}Re_L^{1/2}\right)$ on the buoyancy parameter λ andε. The skin friction coefficient increase with the buoyancy parameter λ and ε monotonously. The physical reason is that the combined effect of positive buoyancy force ($\lambda > 0$) and ε implies a favorable pressure gradient, and fluid becomes accelerated, which results in thinner hydrodynamic and thermal boundary layers. In particular, for $\varepsilon = 0.2$ at $\xi = 1.0$, the skin friction coefficient $\left(C_{fx}Re_L^{1/2}\right)$ decreases approximately 82% as λ decreases from 5.0 to 1.0, while for $\varepsilon = 0.8$ at $\xi = 1.0$ the skin friction coefficient $\left(C_{fx}Re_L^{1/2}\right)$ decreases approximately 69% when λ decreases from 5.0 to 1.0.

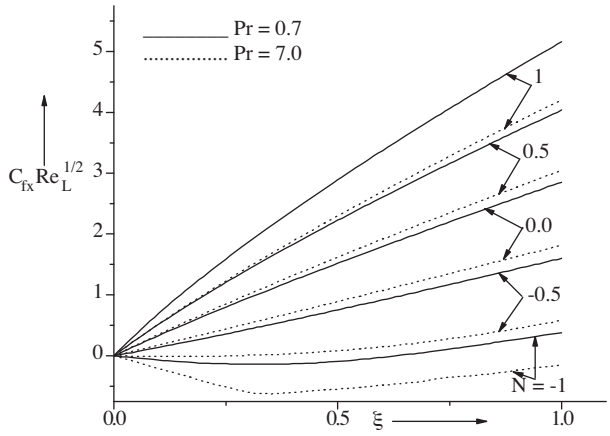

Figure 8. Effects of N and Pr on skin friction coefficient for $\lambda = 2$, $n = 1$, $Q = 0.5$, $\varepsilon = 0.5$, $Sc = 0.22$, and $\Delta = 0.5$.

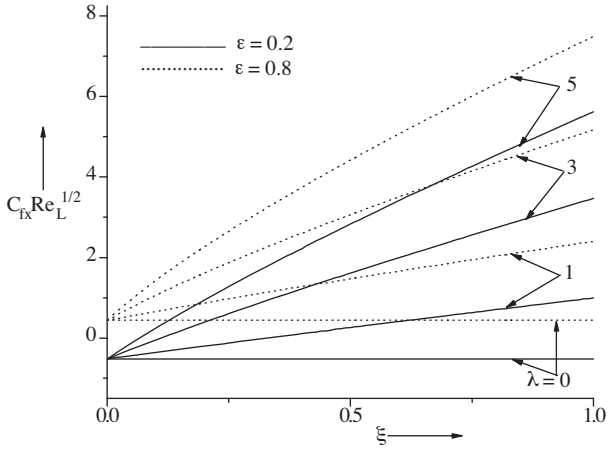

Figure 9. Effects of ε and λ on skin friction coefficient for $Pr = 7.0$, $n = 1$, $Q = 0.5$, $N = 0.5$, $Sc = 0.22$, and $\Delta = 0.5$.

The effects of Prandtl number Pr and heat generation or absorption parameter Qon the heat transfer rate $\left(Nu_x Re_L^{-1/2}\right)$ when $\lambda = 1.0$, $n = 1.0$, $\varepsilon = 0.5$, $Sc = 0.22$, $\Delta = 0.5$, and $N = 1.0$ are shown in Figure 10. It may be noted that negative heat transfer rates are obtained for $Q > 0$. Negative values of - $\Theta'(\xi, 0)$ indicate that heat is transferred from the fluid to the moving surface in spite of the excess of surface temperature over that of the free stream fluid. The physical reason is that for heat generation($Q > 0$), the fluid particles are heated within the boundary layers and the heat transfer rate at the wall becomes negative when fluid particles near the wall reach higher temperature than the surface temperature. Further, it is observed that the positive heat transfer rates $\left(Nu_x Re_L^{-1/2}\right)$ are obtained for heat absorption Q (< 0) and increased monotonously with increasingξ. This is evident from the fact that negative values of Q (< 0) would cause an enlargement of temperature difference between the moving surface and the convective fluid, and thus enhance the heat transfer rate. In particular, for $Q = 0.25$ at $\xi = 1.5$, the heat transfer rate $\left(Nu_x Re_L^{-1/2}\right)$ decreases approximately 101% as the Prandtl number Pr decreases from 7.0 to 0.7, while for $Q =$ –0.25 at $\xi = 1.5$, the heat transfer rate $\left(Nu_x Re_L^{-1/2}\right)$ decreases approximately 63% when the Prandtl number Pr decreases from 7.0 to 0.7. Furthermore, the heat transfer rates are steady when there is no effect of heat generation or absorption ($Q > 0$).

The effects of the chemical reaction parameter Δ and the order of the chemical reaction parameter $n$on the mass transfer rate $\left(Sh_x Re_L^{-1/2}\right)$ when $\lambda = 2.0$, $Pr = 0.7$, $\varepsilon = 0.5$, $Q = 0.5$, $Sc = 0.22$, and $N = 1.0$ are presented in Figure 11. It is observed that the mass transfer rate $\left(Sh_x Re_L^{-1/2}\right)$ decreases (the concentration between the wall and the fluid decreases) when the chemical reaction order n is increased. This is due to the fact that as n ($n = 1, 2, 3$ ...) increases, the power of Φ in the chemical reaction term increases. As the power of Φincreases, the effect of the chemical reaction as a source ($\Delta = 0.5$) weakens, while it is noted that negative mass transfer rates are obtained for $\Delta < 0$. In particular, for $\Delta = 0.5$ at $\xi = 1.5$, the mass transfer rate $\left(Sh_x Re_L^{-1/2}\right)$ increases approximately 15% as the order of the chemical reaction parameter n decreases

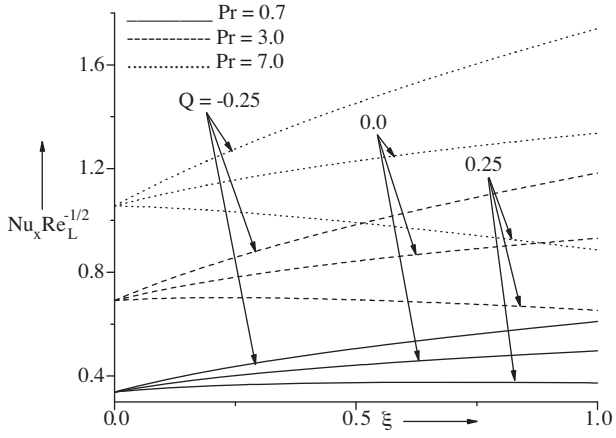

Figure 10. Effects of Q and Pr on heat transfer rate for $\varepsilon = 0.5$, $n = 1$, $\lambda = 1$, $N = 1$, $Sc = 0.22$, and $\Delta = 0.5$.

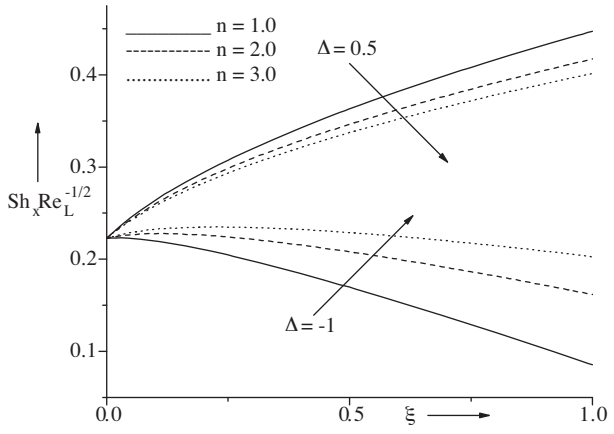

Figure 11. Effects of Δ and Sc on mass transfer rate for $\varepsilon = 0.5$, $Q = 0.5$, $\lambda = 2$, $N = 1$, $n = 1$, and $Pr = 7.0$.

from 3.0 to 1.0, while for $\Delta = -1.0$ at $\xi = 1.5$, the mass transfer rate $\left(Sh_x Re_L^{-1/2}\right)$ decreases approximately 144% when the order of the chemical reaction parameter n decreases from 3.0 to 1.0. It is a clear indication that the destructive chemical reaction impact is more pronounced on the concentration field.

The effects of the Schmidt number Sc and chemical reaction parameter Δ on the mass transfer rate $\left(Sh_x Re_L^{-1/2}\right)$ are depicted in Figure 12. It is noted that the mass transfer rate $\left(Sh_x Re_L^{-1/2}\right)$ is steady for the Schmidt number Sc with a constructive chemical reaction rate ($\Delta = 0.5$), while for a destructive chemical reaction rate ($\Delta = -1.0$) the mass transfer rate $\left(Sh_x Re_L^{-1/2}\right)$ slightly increases on the wall and away from the wall it decreases monotonously with increasing Schmidt number Sc. In particular, for $\Delta = 0.5$ at $\xi = 1.5$, the mass transfer rate $\left(Sh_x Re_L^{-1/2}\right)$ decreases approximately 68% as the Schmidt number Sc decreases from 2.57 to 0.22, while for $\Delta = -1.0$ at $\xi = 1.5$ the mass transfer rate $\left(Sh_x Re_L^{-1/2}\right)$ decreases approximately 92% when the Schmidt number Sc decreases from 2.57 to 0.22.

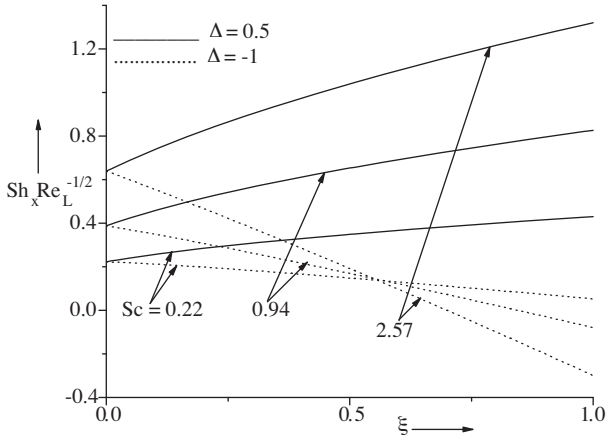

Figure 12. Effects of Δ and Sc on mass transfer rate for $\varepsilon = 0.5$, $Q = 0.5$, $\lambda = 2$, $N = 1$, $n = 1$, and $Pr = 7.0$.

Conclusions

A detailed numerical study has been carried out for the double diffusive mixed convection flow over a moving vertical plate in the presence of internal heat generation or absorption and a homogeneous nth order chemical reaction. Conclusions of the study are as follows:

1. The buoyancy parameter λ and the ratio of buoyancy forces N cause overshoot in the velocity profile for a lower Prandtl number fluid (air, $Pr = 0.7$) but for a higher Prandtl number fluid (water, $Pr = 7.0$) the velocity overshoot is not present.

2. The effect of ε on the velocity profile is significant.

3. Higher Prandtl number $Pr = 7.0$ (water) causes a thinner thermal boundary layer in the presence of heat generation or absorption ($Q > 0$ or $Q < 0$).

4. The heat generation effect ($Q > 0$) causes thicker velocity and thermal boundary layers while the heat

absorption effect ($Q < 0$) has the tendency to reduce the thickness of velocity and thermal boundary layers.

5. Negative heat transfer rates are obtained for $Q > 0$.
6. Chemical reaction parameter Δ and Schmidt number Sc are reducing the concentration boundary layer.
7. Order of the chemical reaction parameter n causes a thicker concentration boundary layer.

Nomenclature

C, D	species concentration and mass diffusivity, respectively
C_W	concentration at the wall
C_∞	species concentration far from the surface
C_{fx}	local skin friction coefficient
C_p	specific heat at constant pressure
f	dimensionless stream function
g	acceleration due to gravity
Gr, Gr^*	Grashof numbers due to temperature and concentration, respectively
k	thermal conductivity
k_1	chemical reaction rate
L	characteristic length
n	order of chemical reaction
N	ratio of Grashof numbers
Nu_x	local Nusselt number
Pr	Prandtl number
Q_0	heat generation coefficient
Q	heat generation or absorption parameter
Re_L	Reynolds number
Sc	Schmidt number
Sh_x	Sherwood number
T	temperature
T_∞	temperature of fluid far away from the wall
T_W	temperature at the wall
U	composite reference velocity
U_w	moving plate velocity
U_∞	free stream velocity
u	velocity component in x-direction
v	velocity component in y-direction

Greek symbols

α	thermal diffusivity
β_T, β_C	volumetric coefficients of the thermal and concentration expansions, respectively
ξ, η	transformed variables
λ, λ_1	buoyancy parameters due to temperature and concentration gradients, respectively
Δ	chemical reaction parameter
Θ	dimensionless temperature
Φ	dimensionless concentration
μ	dynamic viscosity
ν	kinematic viscosity
ρ	density
ψ	stream function

Subscripts

w, ∞	conditions at the wall and infinity, respectively
ξ, η	denote the partial derivatives w.r.t. these variables, respectively
C, T	concentration and temperature

References

Abdelhafez, T.A., "Skin Friction And Heat Transfer on a Continuous Flat Surface Moving in a Parallel Free Stream", Int. J. Heat Mass Transfer 28, 1234-1237, 1985.

Abraham, J.P and Sparrow, E.M., "Friction Drag Resulting from Simultaneous Imposed Motions of a Free Stream and Its Bounding Surface", Int. J. Heat Fluid Flow, 26, 289-295, 2005.

Afzal, N., Baderuddin, A. and Elgarvi, A.A., "Momentum and Heat Transport on a Continuous Flat Surface Moving in a Parallel Stream", Int. J. Heat Mass Transfer 36, 3399-3403, 1993.

Blasius, H., "Grenzschichten in Flussigkeiten mit kleiner Reibung". Z. Math Phys, 56, 1-37, 1908.

Chappidi, P.R. and Gunnerson, F.S., "Analysis of Heat and Momentum Transport along a Moving Surface", Int. J. Heat Mass Transfer, 32, 1383- 1386, 1989.

Cortell, R., "Flow and Heat Transfer in Moving Fluid over a Moving Flat Surface", Theor. Comput. Fluid Dyn., 21, 435-446, 2007.

Ishak, A., Nazar, R. and Pop, I., "The Effects of Transpiration on the Flow and Heat Transfer over a Moving Permeable Surface in a Parallel Stream", Chemical Engineering Journal, 148, 63-67, 2009.

Ishak, A., Nazar, R. and Pop, I., "Boundary Layer Flow over a Continuously Moving Thin Needle in a Parallel Stream", Chinese Physics Letters, 24, 2895-2897, 2007.

Ishak, A., Nazar, R. and Pop, I., "Flow and Heat Transfer Characteristics in a Moving Flat Plate in a Parallel Stream with Constant Surface Heat Flux", Heat Mass Transfer, 4, 563-567, 2009.

Inouye, K. and Tate, A., "Finite Difference Version Quasilinearisation Applied to Boundary Layer Equations", AIAA J., 12, 558-560, 1974.

Lin, H.T. and Haung, S.F., "Flow and Heat Transfer of Plane Surface Moving in Parallel and Reversely to the Free Stream", Int. J. Heat Mass Transfer, 37, 333-336, 1994.

Ostrach, S., "Natural Convection with Combined Driving Forces", Physico Chem Hydrogen, 1, 233-247, 1980.

Roy, S. and Saikrishnan, P., "Non-uniform Slot Injection (Suction) into Steady Laminar Boundary Layer Flow over a Rotating Sphere", Int. J. Heat Mass Transfer, 46, 3389-3396, 2003.

Sakiadis, B.C., "Boundary Layer Behavior on Continuous Solid Surfaces: II. Boundary Layer on a Continuous Flat Surface", AIChE J., 7, 221-225, 1961.

Schlichting, H., "Boundary Layer Theory", Springer, New York, 2000.

Sparrow, E.M. and Abraham, J.P., "Universal Solutions for the Stream Wise Variation of the Temperature of a Moving Sheet in the Presence of a Moving Fluid", Int. J. Heat Mass Transfer, 48, 3047-3056, 2005.

Tsou, F., Sparrow, E. and Goldstein, R., "Flow and Heat Transfer in the Boundary Layer on a Continuous Moving Surface", Int. J. Heat Mass Transfer, 10, 219-235, 1967.

Varga, R.S., "Matrix Iterative Analysis", Prentice Hall, 2000.

Viskanta, R., Bergman, T.L. and Incropera, F.P., "Double Diffusive Natural Convection". in: Kakac, S., Aung, W. and Viskanta, R., (eds) Natural Convection: Fundamentals and Applications. Hemisphere, Washington, 1075-1099, 1985.